行政院國家科學委員會專題研究計畫 成果報告

Silibinin抑制不同腎臟癌細胞株(Caki-1, Caki-2, 786-0)轉移及侵襲之機制探討(第2年)
研究成果報告(完整版)

計 畫 類 別 ：個別型
計 畫 編 號 ：NSC 96-2314-B-040-006-MY2
執 行 期 間 ：97年08月01日至98年07月31日
執 行 單 位 ：中山醫學大學醫學系

計 畫 主 持 人：張浤榮
共 同 主 持 人：謝易修
計畫參與人員：碩士班研究生-兼任助理人員：孫瑛穗

處 理 方 式 ：本計畫涉及專利或其他智慧財產權，1年後可公開查詢

中 華 民 國 98年10月31日

Silibinin Inhibits the Invasion and Migration of Renal Cell Carcinoma Cells in Vitro and in Vivo and Enhances the Cytotoxic Effects of Anti-cancer Agents

Horng-Rong Chang[a,b], Shun-Fa Yang[b], Jong-Da Lian[a], Yih-Shou Hsieh[c]

[a]Division of Nephrology, Department of Internal Medicine, Chung Shan Medical University Hospital, Taichung 402, Taiwan

[b]Institute of Medicine, Chung Shan Medical University, Taichung 402, Taiwan

[c]Institute of Biochemistry and Biotechnology, Chung Shan Medical University, Taichung 402, Taiwan

Corresponding Author:

Yih-Shou Hsieh, Ph.D.

Institute of Biochemistry and Biotechnology, Chung Shan Medical University, Taichung 402, Taiwan

Tel.: +886-4-24730022 ext 11678; Fax: +886-4-23248195

E-mail: csmcysh@csmu.edu.tw

Abstract

Cancer metastasis, involving multiple processes and various cytophysiological changes, is a primary cause of cancer death and may complicate the clinical management, even lead to death. Silibinin is a flavonoid antioxidant and wildly used for its antihepatotoxic properties and recent studies have revealed pleiotropic anticancer and antiproliferative capabilities of silibinin. In this study, we first observed that silibinin exerted a dose-dependent inhibitory effect on the invasion and motility of 786-O renal cell carcinoma cells in the absence of cytotoxicity. To look at the precise involvement of silibinin in cancer metastasis, 786-O cells were treated with silibinin at various concentrations, up to 50 μM, for a defined period and then subjected to gelatin zymography, casein zymography and western blot to investigate the impacts of silibinin on metalloproteinase-2, -9, urokinase plasminogen activator (u-PA), and MAPK pathway signaling protein, respectively. The results showed that silibinin treatment decreased the expressions of MMP-2 and u-PA in a concentration-dependent manner and decrease the expression of p-p38 and p-Erk1/2. Thus, silibinin may possess an anti-metastatic activity in 786-O renal cell carcinoma cells. To further evaluate the anti-tumor effect of silibinin, an *in vivo* anti-tumor study using nude mice xenograft model by a subcutaneous inoculation of RCC 786-O cells was performed. Small solid tumors was observed on 8 days following cell inoculation and a 70.1% reduction of tumor volume by silibinin feeding was seen on day 44, compared to control animals.

Keywords: matrix metalloproteinase, MMP-2, u-PA, TIMP-2

Introduction

Renal cell carcinoma (RCC) is the most common malignancy of the kidney and accounts for approximately 3% of adult cancers (1). RCC arises from the renal epithelium and account for about 85 percent of renal cancers. RCC is more common in men than in women (ratio 2:1), the median age at diagnosis is approximately 60 years. Approximately 2% of cases of renal cancer are associated with inherited syndromes. Surgical resection (nephrectomy and partial nephrectomy) is the preferred treatment for localized primary tumors in patients with stage I through stage IV disease, but surgical cure of disease is strongly dependent on stage and grade of disease. A quarter of the patients present with advanced disease, including locally invasive or metastatic renal-cell carcinoma. The median survival for patients with metastatic disease is about 13 months.

Medical therapies are generally offered for locally advanced or metastatic RCC. The rates of response to chemotherapy alone are low (roughly 4%-6 %) (2, 3). Immunomodulatory therapies with a variety of cytokines have been studied in patients with metastatic RCC. Two of these agents, interleukin 2 and interferon-α, have reproducible antitumor effects with objective response rates of 15% to 31%. However, the majority of patients with metastatic RCC do not benefit from these therapies (4). Until 2005, only a single treatment, high dose interleukin-2, had been approved by the Food and Drug Administration (FDA) for the treatment of this disease (5).

Metastatic RCC has a poor overall survival. About 20%-30% patients who present with limited disease at the time of nephrectomy develop metastasis. The median time to relapse after nephrectomy is 15-18 months. The maximum numbers of relapses are within the first 3 years (4, 6). In metastatic RCC, high dose immunotherapy with intravenous interleukin-2 results in generally durable complete responses in approximately 6% of patients, but this treatment is associated with significant toxicity (7). Recently there has been an improved understanding of the biology of RCC. This has lead to the development of various agents that target ligands at the molecular level. The hypoxia inducible factor-alfa (HIF-α)/vascular endothelial growth factor (VEGF) pathway and mammalian target of rapamycin (mTOR) signal transduction pathway are targets for some of these novel agents. Compelling evidence has demonstrated VHL inactivation in the majority of clear cell RCC tumors leading to VEGF overexpression will drive tumor angiogenesis. Inhibition of VEGF has been pursued as a therapeutic target in metastatic RCC (8). A number of randomized phase III trials have shown an improved outcome in patients with metastatic disease who received these targeted agents (9-11).

Silibinin is a flavonoid antioxidant and wildly used for its anti-hepatotoxic properties and recent evidence over the past decade has demonstrated that silibinin possesses pleiotropic anticancer and antiproliferative capabilities in different tumor cells, including prostate (12, 13), skin (14, 15), colon (16), osteosarcoma (17) and bladder cancer models (12-18). In *in vitro*

studies, silibinin strongly inhibits cell growth and DNA synthesis to cause cell cycle arrest and apoptotic cell death through an activated caspase cascade (19, 20). Silibinin is exceptionally well tolerated and largely free of adverse effects (21) and mice fed with silibinin (up to 2 g/kg) do not show any apparent signs of toxicity (22). Due to its excellent safety profile, anticancer activity, well-known pharmacokinetics and widespread tissue distribution, silibinin has been considered a suitable candidate for cancer chemotherapy and chemoprevention (23-25). Thus, we conducted this study to investigate whether silibinin is with an inhibitory effect on the invasion and migration of 786-O RCC cells.

Materials and methods

Cell Culture and Silibinin Treatment

The RCC cell line 786-0 and the HEK-293 (human embryonic kidney) cell were purchased from the Food Industry Research and Development Institute (Hsinchu, Taiwan). The RCC cell line 786-0 was cultured in RPMI 1640 medium supplemented with 10% fetal calf serum, 2 mM L-glutamine, 100 μg/ml streptomycin, and 100 units/ml penicillin and the HEK-293 cell line was cultured in minimum essential medium (Gibco) containing 10% horse serum. The cell cultures were maintained at 37°C in a humidified atmosphere of 5% CO_2. For silibinin treatment, appropriate amounts of stock solution [0.1 M in dimethyl sulfoxide (Merck, Darmstadt, Germany)] of silibinin (Sigma) were added into culture medium to achieve the indicated concentrations and then incubated with cells for indicated time periods, whereas dimethyl sulfoxide solution (final Conc. 0.1% DMSO) without silibinin was used as blank reagent.

Determination of cell viability (MTT assay)

To evaluate the cytotoxicity of silibinin, a MTT colorimetric assay was performed to determine the cell viability (26). Cells were seeded in 24-well plates at a density of 3.5 x 10^4 cells/well and treated with silibinin at 0-50 μM concentration at 37℃ for 24 h. After the exposure period, media were removed, followed by washing of the cells with PBS. Thereafter, the medium was changed and incubated with 20 μL MTT (5 mg/mL) for 4 h. The viable cell

number/dish is directly proportional to the production of formazan, which following solubilization with isopropanol, can be measured spectrophotometrically at 563 nm.

Cell Invasion and Motility Assays

After a treatment with silibinin (0, 5, 10, 20, and 50 μM) for 24 hrs, cells were harvested and seeded in a Boyden chamber (Neuro Probe, Cabin John, MD, USA) with 10^4 cells/well in serum-free medium, and then incubated for 48 hrs at 37°C. For the invasion assay, 10 μL Matrigel (25 mg/50 mL; BD Biosciences, Bedford, MA, USA) was applied to 8-μm-pore-size polycarbonate membrane filters, and the bottom chamber of the apparatus contained standard medium. Following incubation, filters were then air-dried for 5 hrs in a laminar flow hood. The invaded cells were fixed with methanol and stained with Giemsa. Cell numbers were counted under a light microscope. The motility assay was carried out as described for the invasion assay, with no coating of Matrigel (27).

Determination of MMP-2, MMP-9 and u-PA by Zymography

The activities of MMP-2 and MMP-9 of the condition medium were measured by gelatin-zymogram protease assays as previously described (28). Briefly, samples were prepared with standard SDS-gel-loading buffer containing 0.01% SDS without β-mercaptoethanol and not boiled before loading. Then, prepared samples were subjected to electrophoresis with 8% SDS polyacrylamide gels (0.75-mm thick, acrylamide/bis-acrylamide = 30/1.2) containing 0.1% gelatin. Electrophoresis was performed

at 150 V for 3 h in an OWL P-1 apparatus. After electrophoresis, gels were washed twice with 100 mL distilled water containing 2% Triton X-100 on a gyratory shaker for 30 min at room temperature to remove SDS. The gel was then incubated in 100 mL reaction buffer (40 mM Tris-HCl, pH 8.0, 10 mM $CaCl_2$, 0.02% NaN_3) for 12 h at 37℃, stained with Coomassie brilliant blue R-250 and destained with methanol-acetic acid-water (50/75/875, v/v/v).

Visualization of u-PA activity was performed as previously described (28). Briefly, 2% w/v casein and 20 μg/mL plasminogen were added to 8% SDS-PAGE gels, and then electrophoresis and zymography were performed as described in the gelatin zymography.

Immunoblotting

Samples of cell lysates or nuclear fractions were separated in a 12.5% polyacrylamide gel and transferred onto a nitrocellulose membrane as previously described (28). The blot was subsequently treated by standard procedures and probed with ERK1/2, p38, JNK1/2, and Akt, the total and phosphorylated proteins (Biosource, Camarillo, CA, USA), and NF-κB, c-Jun, c-Fos, C23 (BD Transduction Laboratories, San Diego, CA, USA), TIMP-2 (Serotec, Oxford, UK), and PAI-1 (American Diagnostics Inc., Greenwich, CT, USA) antibodies. The protein expression was detected by chemiluminescence with an ECL Plus detection kit (Amersham Life Sciences, Inc., Piscataway, NJ, USA).

Reverse Transcription-Ploymerase Chain Reaction (RT-PCR)

For reverse transcription, 2 μg of total ribonucleic acid (RNA) were used as templates in a 20 μl reaction containing 4 μl dNTPs (2.5 mM), 2.5 μl Oligo dT (10 pmole/μL) and 200U RTase. The appropriate primers [5'-GGCCCTGTCACTCCTGAGAT-3' and 5'-GGCATCCAGGTTATCGGGGA-3' for MMP-2 (473bp), 5'-CAACATCACCTATTGGATCC -3' and 5'- CGGGTGTAGAGTCTCTCGCT for MMP-9 (479bp), 5'-TTGCGGCCATCTACAGGAG-3' and 5'-ACTGGGGATCGTTATACATC-3' for u-PA (351bp), and 5'-CGGAGTCAACGGATTTGGTCGTAT-3' and 5'-AGCCTTCTCCATGGTTGGTGAAGAC-3' for GAPDH (305bp)] were used for PCR amplifications. PCR was performed using Platinum Taq polymerase (Invitrogen) as bellow condition: 25 cycles of 94°C for 1 min, 55°C (u-PA) or 63°C (MMP-2, MMP-9 and GAPDH) for 1 min, 72°C for 2 minutes followed by 10 min at 72°C.

Electrophoretic Mobility Shift Assay

AP-1- and NF-κB-binding assays in nuclear extracts were performed with biotin-labeled double-stranded AP-1 or NF-κB oligonucleotides (Promega, Madison, WI), and the electrophoretic mobility shift assay was carried out by using the Lightshift kit (Promega). Briefly, binding reactions containing 10 μg of nuclear protein, 10 mM Tris, 50 mM KCl, 1 mM dithiothreitol, 5 mM $MgCl_2$, 2 μg poly (dI·dC) and 2 pmol of oligonucleotide probe were incubated for 20 min at room temperature. Protein DNA complexes were separated by electrophoresis on a 6% non-denaturing acrylamide gel, transferred to positively charged

nylon membranes and then cross-linked in a Stratagene cross-linker. Gel shifts were visualized with a streptavidin–horseradish peroxidase followed by chemiluminescent detection.

Measurement of tumor growth in nude mice

For nude mice xenograft model, male immunodeficient nude mice (ICR *nu*/*nu* mice) of 5-6-weeks old with a weight of 18-22 g were used. Mice were housed with a regular 12-h light/12-h dark cycle and *ad libitum* access to standard rodent chow diet (Laboratory Rodent Diet 5001, LabDiet, St. Louis, MO), and kept in a pathogen-free environment at the Laboratory Animal Unit. RCC 786-O cells (5×10^6 cells/0.2 mL/mouse) were injected subcutaneously into the right front axilla. After xenograft implantation, mice were randomly divided into three groups ($N = 5$ for each group) to be fed by oral gavage with saline (control) and silibinin (100 mg/day/kg and 200 mg/day/kg) suspended in saline. The day of cell implantation was designanted day 0 and tumor growth and tumor appearance were assessed daily after cell injection. After 44 days, animals were euthanized, and the primary tumors were isolated and weighed.

Statisical Analysis

For all of the measurements, analysis of variance followed by Scheffe posteriori comparison was used to assess the differences between control and cells treated with various concentration of silibinin. The Student's *t*-test was used to analyze the difference between control and

silibinin-treated cells after overexpression of constructively active MEK1. Statistical significance was set at $P < 0.05$.

Statistical significances of difference throughout this study were calculated by Student's *t* test (SigmaStat 2.0, Jandel Scientific, San Rafael, CA, USA).

Results

Absence of Cytotoxicity of silibinin on HEK-293 cells and RCC 786-O cells

RCC 786-O cell viabilities in the presence of 0, 5, 10, 20 and 50 μM silibinin were not significantly different to that of controls in the microculture tetrazolium assay (Figure 1A) ($P > 0.05$). We have also described the absence of cytotoxic effect of silibinin up to 100 μM on human lung cancer A549 cells previously (28). Thus, we used this concentration range for silibinin in all subsequent experiments. The result of the same experiment on a human embryonic kidney cell line (HEK-293 cells) was similar to that with 786-O cell (Figure 1B).

Inhibition on Invasion and Motility of RCC 786 -O Cells by Silibinin

With a cell invasion assay with Boyden chamber coated with Matrigel, it was shown that silibinin significantly reduced the invasion of RCC 786-O cells because only as low as 47.8± 4.9% ($P<0.001$) of invasion capability was retained after a treatment with 50 μM silibinin. Such reduction was concentration-dependent (Figure 2). Moreover, the inhibitory effect, also in a concentration-dependent manner, of silibinin on cell migration as observed with76.1± 5.6% left after a 50 μM silibinin treatment ($P<0.01$) (Figure 2).

Silibinin suppressed the expression and activity of MMP-9, MMP-2 and u-PA in RCC 786-O cells

Because extracellular matrix degradation is crucial to cellular invasion, suggesting that

matrix-degrading proteinases are required, to clarify if MMPs and u-PA are involved in inhibition of invasion and motility by silibinin, the effects of silibinin on MMPs and u-PA activities were investigated by gelatin and casein zymography under a condition of serum starvation, respectively. As results shown in Figure 3A, silibinin reduced the level of u-PA in casein zymography ($P < 0.001$), the level of MMP-2 ($P < 0.001$) and the level of MMP-9 ($P < 0.001$) in gelatin zymography. Silibinin also reduced the levels of MMP-9 ($P < 0.001$), MMP-2 ($P < 0.001$) and u-PA ($P < 0.001$) in western blotting in a dose-dependent manner (Figure 4A). Furthermore, if the regulatory effects of silibinin on proteases were on the mRNA levels was evaluated by semi-quantitative RT-PCR analysis. With glyceraldehyde-3-phosphate dehydrogenase (GAPDH) as an internal control, mRNA levels of MMP-2, MMP-9, and u-PA were significantly reduced in 786-O cells (Fig 3B).

Silibinin Exerted a Stimulatory Effect on the Protein Levels of TIMP-2 and PAI-1

Plasminogen activator inhibitor-1 (PAI-1), the major circulating PAI, controls the rate of plasmin generation by forming irreversible inhibitory complexes with u-PA (29). Physiological activity of MMP-2 is greatly related to that of tissue inhibitors of metalloproteinases-2 (TIMP-2), a specific endogenous inhibitor, therefore we performed a western blot to see the effect of silibinin on expression of PAI-1 and TIMP-2. The results showed that along with a gradual increase in the concentration of silibinin 0, 5, 10, 20 and 50

μM for 24 h, both of the TIMP-2 and PAI-1 protein level (TIMP-2: $P < 0.01$, Erk2: $P < 0.001$) were gradually increased in western blotting as shown in Figure 4B.

Silibinin inhibited the phosphorylation of ERK 1/2 and p38 in RCC 786-O cells

Western blots showed that silibinin significantly inhibited the phosphorylation of p38 ($P < 0.001$) (Figure 5A) and Erk 1/2 (Erk1: $P < 0.001$, Erk2: $P < 0.001$) (Figure 5B) in RCC 786-O cells in a dose-dependent manner, but had no effect on the phosphorylation of JNK 1/2 (Figure 5C) and Akt (Figure 5D).

Silibinin decreased NF-κB, c-Jun and c-fos and activation in RCC 786-O cells

In western blotting, silibinin significantly inhibited the levels of NF-κB, c-Jun and c-Fos in nuclear extracts of RCC 786-O cells in a dose-dependent manner ($P < 0.001$) (Figure 6A). Electrophoretic mobility shift assay showed that silibinin inhibited the DNA-binding activity of AP-1 and NF-κB in RCC 786-O cells (Figure 6B & 6C).

Silibinin suppressed the tumor growth in RCC 786-O xenograft nude mice

To further evaluate the anti-tumor effect of silibinin, an *in vivo* anti-tumor study using nude mice xenograft model by a subcutaneous inoculation of RCC 786-O cells was performed. Small solid tumors was observed on 8 days following cell inoculation and a 70.1% reduction of averaged tumor volume (490±79.3 mm^3) by silibinin 200 mg/kg feeding was seen on day 44, compared to that of control animals (1640±223.3 mm^3) (Fig. 7A). Moreover, by Day 44, silibinin (200 mg/kg) feeding induced a 3.3-fold ($P < 0.001$) reduction in tumor weight (Fig.

7B). There were no apparent signs of toxicity of silibinin by diet consumption an d body weight monitoring throughout the experiment (Fig. 7C).

Discussion

In this report, we demonstrate that (i) silibinin suppresses cellular migration and invasion of RCC 786-O cells, accompanied by a decrease in u-PA, MMP-2 and MMP-9 expression and an increase of PAI-1 and TIMP-2; (ii) the mechanism may involve the inhibition of p38- and ERK-dependent NF-κB and AP-1 induction, but does not involve JNK and Akt pathways; (iii) the nude mice xenograft model by subcutaneous inoculation of RCC 786-O cells also demonstrated a anti-tumor effect of silibinin.

The matrix metalloproteinases (MMP) and the plasminogen activation system play crucial roles in the process of cancer invasion and metastasis. Serine proteases, metalloproteases and their inhibitors are key enzymes involved in matrix remodeling during cancer invasion, metastasis and angiogenesis. MMP-2, MMP-9, and tissue inhibitors of metalloproteinases -1, -2 (TIMP-1, TIMP-2) have been found to be of prognostic significance in HCC. In the present study, treatment with silibinin inhibited the expression of u-PA, MMP-2 and MMP-9 in a dose-dependent manner in 786-O, suggesting that this down-regulation of u-PA, MMP-2 and MMP-9 contributes to the reduction of the invasion of 786-O cells.

In several tumor types, elevated levels of urokinase plasminogen activator (uPA), its receptor (uPAR) or its inhibitor plasminogen activator inhibitor-1 (PAI-1) is associated with a poorer prognosis. uPA activity may be the most sensitive factor affecting HCC invasion in the plasminogen activation system and is a strong predictor for the recurrence and prognosis of HCC. The PAI-1 proteinis a multifaceted proteolytic factor. It not only functions as an inhibitor of the protease uPA, but also plays an important role in signal transduction, cell adherence, and cell migration. Thus, an apparent paradox cons idering its name-although it inhibits uPA during blood coagulation, it actually promotes invasion and metastasis. In many malignancies including HCC, elevated PAI-1 is associated with tumor aggressiveness and poor patient outcome.

In conclusion, our observations indicate silibinin has an inhibitory effect on several essential steps of metastasis, including cell invasion and migration. In addition, silibinin could regulate the activities of invasion-associated proteinases. As evidenced from above results, silibinin may be a powerful candidate for a preventive agent against 786-O renal cell carcinoma cancer metastasis.

Acknowledgment

This study was supported by a research grant from National Science Council, Republic of China (National Science Council 96-2314-B-040-006-MY2).

Figure Legends

Figure 1. Effects of silibinin on cell viability of 786-O (A) and HEK-293 (B) cells. After being treated with silibinin at a concentration of 0, 5, 10, 20 or 50 μM for 24 hours, MTT assay were then performed.

Figure 2. Effects of silibinin on cell invasion and migration of 786-O cell. After being treated with silibinin at a concentration of 0, 5, 10, 20 or 50 μM for 24 hours, cell invasion (A) and migration (B) assay were then performed. The values represented the mean ± SD of at least 3 independent experiments (*, $P<0.05$; **, $P<0.01$; ***, $P<0.001$).

Figure 3. Effects of silibinin on the activities and mRNA levels of MMP-2, MMP-9 and u-PA. (A) 786-O cells were treated with 0, 5, 10, 20 or 50 μM of silibinin for 24 hours and then subjected to gelatin zymography and western blotting to analyze the activities and levels of MMP-2 and u-PA, respectively. (B) For mRNA levels, 786-O total RNAs were extracted and subjected to a semi-quantitative RT-PCR for MMP-9, MMP-2 and u-PA with GAPDH being an internal control.The values represented the mean ± SD of at least 3 independent experiments (*, $P<0.05$; **, $P<0.01$; ***, $P<0.001$).

Figure 4. Effects of silibinin on the expression of proteases and their endogenous inhibitors.

786-O cells were treated with 0, 5, 10, 20 or 50 μM of silibinin for 24 hours and then subjected to western blotting to analyze the levels of (A) proteases (MMP-2 MMP-9 and u-PA) and (B) their endogenous inhibitors (TIMP-2 and PAI-1), respectively. The values represented the mean ± SD of at least 3 independent experiments (*, $P<0.05$; **, $P<0.01$; ***, $P<0.001$).

Figure 5. Effects of silibinin on the protein levels of the MAPK and PI3K-Akt pathways. 786-O cells were treated with 0, 5, 10, 20 or 50 μM of silibinin for 24 hours, and then cell lysates were subjected to SDS-PAGE followed by western blotting with anti-p-p38 (A), anti-p-Erk1/2 (B), anti-p-JNK1/2 (C) and anti-pAkt (D) antibodies. Signals of proteins were visualized with an ECL detection system. The values represented the mean ± SD of at least 3 independent experiments (*, $P<0.05$; **, $P<0.01$; ***, $P<0.001$).

Figure 6. Effects of silibinin on the activation of NF-κB, c-Jun, and c-Fos. (A)Cells were treated with silibinin and then nuclear extracts were subjected to SDS-PAGE followed by western blotting with anti-NF-κB, c-Fos, c-Jun, or C23 antibodies. Signals of proteins were visualized with an ECL detection system. Nuclear extracts were subjected to DNA binding activity of NF-κB (B) and AP-1 (C) using biotin labeled NF-κB and AP-1 specific oligonucleotide in EMSA. The last lane represented nuclear extracts incubated with unlabeled oligonucleotide (Comp.) to confirm the specificity of binding. The values represented the

mean ± SD of at least 3 independent experiments (**, P<0.01; ***, P<0.001).

Figure 7. The *in vivo* anticancer effects of silibinin. After subcutaneous implantation of 786-O cells, BALB/c *nu/nu* mice were treated with PBS or silibinin as described in Materials and Methods and then analyzed for the growth of tumor (A) the weight of primary tumor (B), and body weight of mice (C). The values represented the means ± SD (***, *P*<0.001).

References

1. Hutson TE. Renal cell carcinoma: diagnosis and treatment, 1994-2003. Proc (Bayl Univ Med Cent) 2005;18(4):337-340.
2. Amato RJ. Chemotherapy for renal cell carcinoma. Semin Oncol 2000;27(2):177-186.
3. Yagoda A, Abi-Rached B, Petrylak D. Chemotherapy for advanced renal-cell carcinoma: 1983-1993. Semin Oncol 1995;22(1):42-60.
4. Cohen HT, McGovern FJ. Renal-cell carcinoma. N Engl J Med 2005;353(23):2477-2490.
5. Brugarolas J. Renal-cell carcinoma--molecular pathways and therapies. N Engl J Med 2007;356(2):185-187.
6. Athar U, Gentile TC. Treatment options for metastatic renal cell carcinoma: a review. Can J Urol 2008;15(2):3954-3966.
7. Rosenberg SA, Yang JC, White DE, Steinberg SM. Durability of complete responses in patients with metastatic cancer treated with high-dose interleukin-2: identification of the antigens mediating response. Annals of surgery 1998;228(3):307-319.
8. Rini BI. VEGF-targeted therapy in metastatic renal cell carcinoma. Oncologist 2005;10(3):191-197.
9. Rini BI, Halabi S, Taylor J, Small EJ, Schilsky RL. Cancer and Leukemia Group B 90206: A randomized phase III trial of interferon-alpha or interferon-alpha plus anti-vascular endothelial growth factor antibody (bevacizumab) in metastatic renal cell carcinoma. Clin Cancer Res 2004;10(8):2584-2586.
10. Motzer RJ, Escudier B, Oudard S, Hutson TE, Porta C, Bracarda S et al. Efficacy of everolimus in advanced renal cell carcinoma: a double-blind, randomised, placebo-controlled phase III trial. Lancet 2008;372(9637):449-456.

11. Hudes G, Carducci M, Tomczak P, Dutcher J, Figlin R, Kapoor A et al. Temsirolimus, interferon alfa, or both for advanced renal-cell carcinoma. N Engl J Med 2007;356(22):2271-2281.

12. Singh RP, Dhanalakshmi S, Tyagi AK, Chan DC, Agarwal C, Agarwal R. Dietary feeding of silibinin inhibits advance human prostate carcinoma growth in athymic nude mice and increases plasma insulin-like growth factor-binding protein-3 levels. Cancer Res 2002;62(11):3063-3069.

13. Singh RP, Agarwal R. Prostate cancer chemoprevention by silibinin: bench to bedside. Mol Carcinog 2006;45(6):436-442.

14. Katiyar SK, Korman NJ, Mukhtar H, Agarwal R. Protective effects of silymarin against photocarcinogenesis in a mouse skin model. J Natl Cancer Inst 1997;89(8):556-566.

15. Singh RP, Agarwal R. Flavonoid antioxidant silymarin and skin cancer. Antioxid Redox Signal 2002;4(4):655-663.

16. Kohno H, Tanaka T, Kawabata K, Hirose Y, Sugie S, Tsuda H et al. Silymarin, a naturally occurring polyphenolic antioxidant flavonoid, inhibits azoxymethane-induced colon carcinogenesis in male F344 rats. Int J Cancer 2002;101(5):461-468.

17. Hsieh YS, Chu SC, Yang SF, Chen PN, Liu YC, Lu KH. Silibinin suppresses human osteosarcoma MG-63 cell invasion by inhibiting the ERK-dependent c-Jun/AP-1 induction of MMP-2. Carcinogenesis 2007;28(5):977-987.

18. Tyagi A, Raina K, Singh RP, Gu M, Agarwal C, Harrison G et al. Chemopreventive effects of silymarin and silibinin on N-butyl-N-(4-hydroxybutyl) nitrosamine induced urinary bladder carcinogenesis in male ICR mice. Mol Cancer Ther 2007;6(12 Pt 1):3248-3255.

19. Mohan S, Dhanalakshmi S, Mallikarjuna GU, Singh RP, Agarwal R. Silibinin modulates UVB-induced apoptosis via mitochondrial proteins, caspases activation, and mitogen-activated protein kinase signaling in human epidermoid carcinoma A431 cells. Biochem Biophys Res Commun 2004;320(1):183-189.

20. Tyagi AK, Singh RP, Agarwal C, Chan DC, Agarwal R. Silibinin strongly synergizes human prostate carcinoma DU145 cells to doxorubicin-induced growth Inhibition, G2-M arrest, and apoptosis. Clin Cancer Res 2002;8(11):3512-3519.

21. Lahiri-Chatterjee M, Katiyar SK, Mohan RR, Agarwal R. A flavonoid antioxidant, silymarin, affords exceptionally high protection against tumor promotion in the SENCAR mouse skin tumorigenesis model. Cancer Res 1999;59(3):622-632.

22. Agarwal C, Singh RP, Dhanalakshmi S, Tyagi AK, Tecklenburg M, Sclafani RA et al. Silibinin upregulates the expression of cyclin-dependent kinase inhibitors and causes cell cycle arrest and apoptosis in human colon carcinoma HT-29 cells. Oncogene 2003;22(51):8271-8282.

23. Lorenz D, Lucker PW, Mennicke WH, Wetzelsberger N. Pharmacokinetic studies with silymarin in human serum and bile. Methods Find Exp Clin Pharmacol 1984;6(10):655-661.

24. Weyhenmeyer R, Mascher H, Birkmayer J. Study on dose-linearity of the pharmacokinetics of silibinin diastereomers using a new stereospecific assay. Int J Clin Pharmacol Ther Toxicol 1992;30(4):134-138.

25. Zhao J, Agarwal R. Tissue distribution of silibinin, the major active constituent of silymarin, in mice and its association with enhancement of phase II enzymes: implications in cancer chemoprevention. Carcinogenesis 1999;20(11):2101-2108.

26. Mosmann T. Rapid colorimetric assay for cellular growth and survival: application to proliferation and cytotoxicity assays. J Immunol Methods 1983;65(1-2):55-63.

27. Chen PN, Chu SC, Chiou HL, Kuo WH, Chiang CL, Hsieh YS. Mulberry anthocyanins, cyanidin 3-rutinoside and cyanidin 3-glucoside, exhibited an inhibitory effect on the migration and invasion of a human lung cancer cell line. Cancer Lett 2006;235(2):248-259.

28. Chu SC, Chiou HL, Chen PN, Yang SF, Hsieh YS. Silibinin inhibits the invasion of human lung cancer cells via decreased productions of urokinase-plasminogen activator and matrix metalloproteinase-2. Mol Carcinog 2004;40(3):143-149.

29. Andreasen PA, Egelund R, Petersen HH. The plasminogen activation system in tumor growth, invasion, and metastasis. Cell Mol Life Sci 2000;57(1):25-40.

Figure 1

(A)

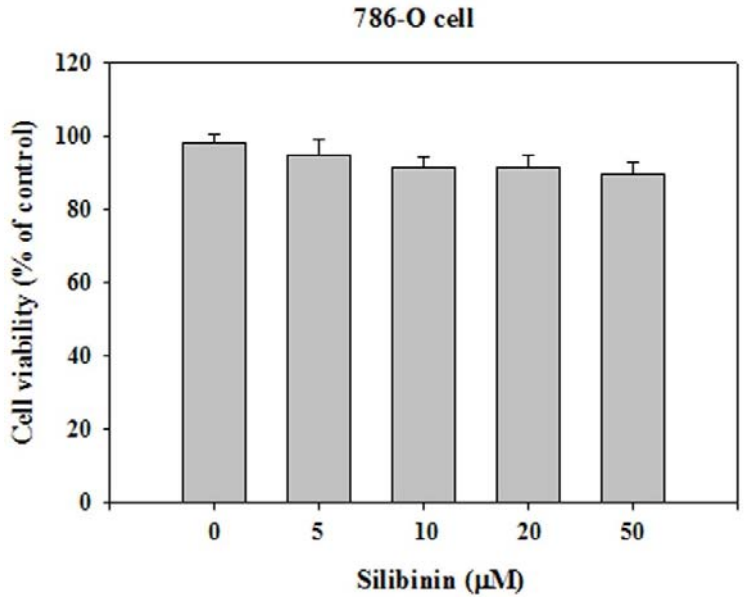
786-O cell
Cell viability (% of control)
120
100
80
60
40
20
0
0
5
10
20
50
Silibinin (μM)

(B)

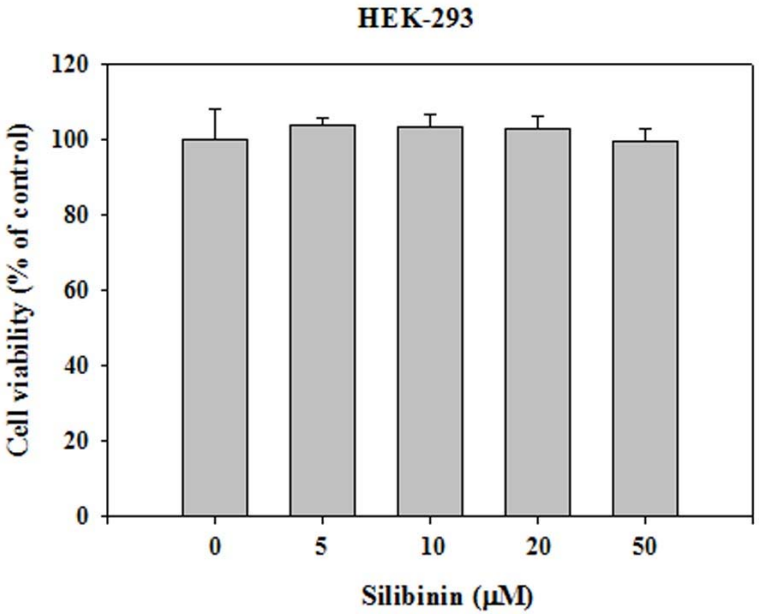
HEK-293
Cell viability (% of control)
120
100
80
60
40
20
0
0
5
10
20
50
Silibinin (μM)

Figure 2

(A)

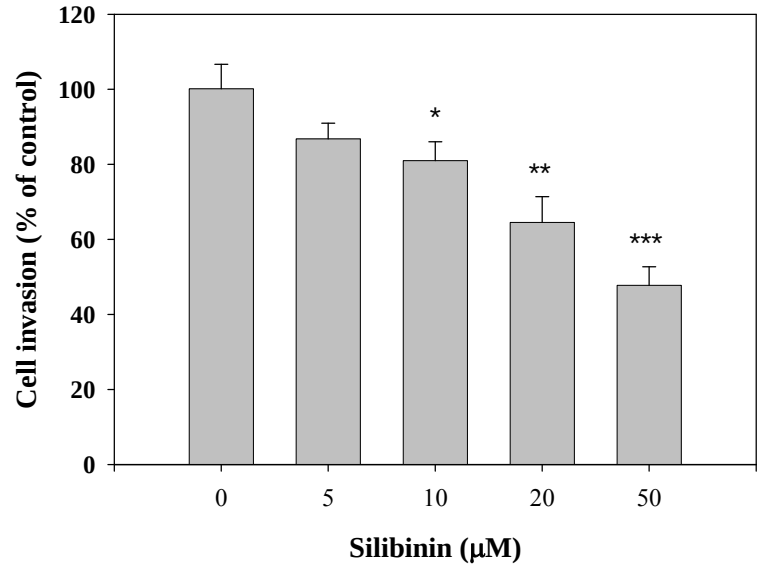
Cell invasion (% of control)
120
100
80
60
40
20
0
*
**
***
0
5
10
20
50
Silibinin (μM)

(B)

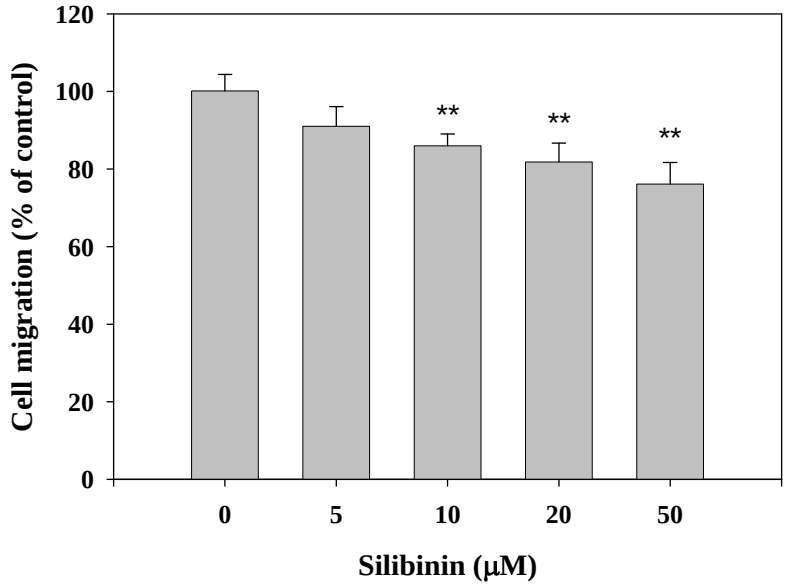
Cell migration (% of control)
120
100
80
60
40
20
0
**
**
**
0
5
10
20
50
Silibinin (μM)

Figure 3

(A)

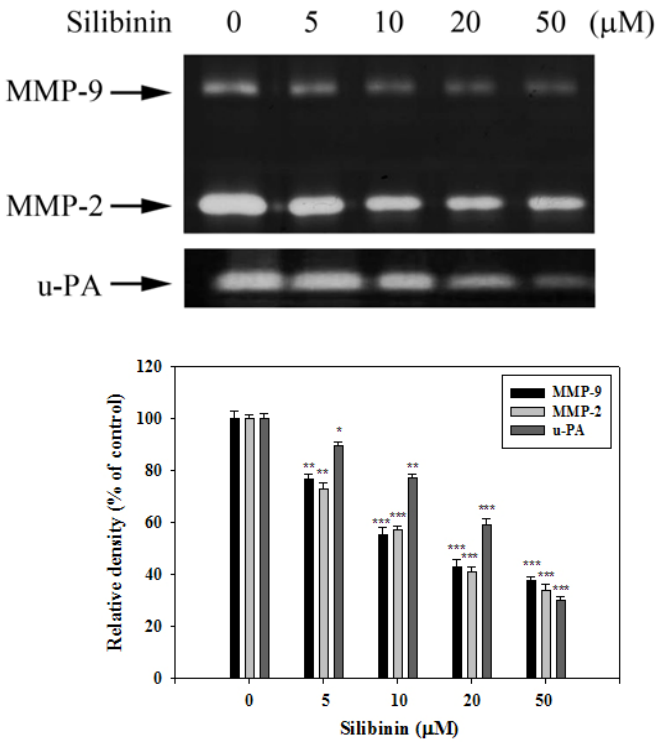
Silibinin 0 5 10 20 50 (μM)
MMP-9
MMP-2
u-PA
Relative density (% of control)
MMP-9
MMP-2
u-PA
Silibinin (μM)

(B)

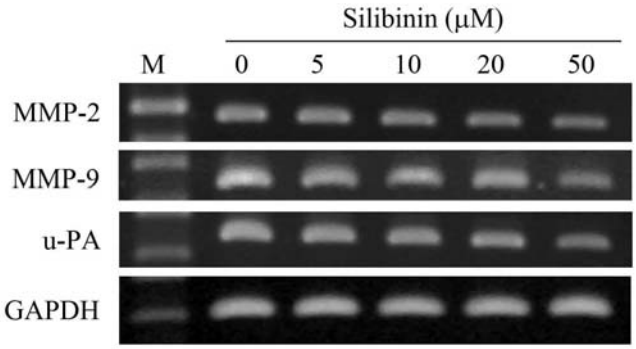
Silibinin (μM)
M 0 5 10 20 50
MMP-2
MMP-9
u-PA
GAPDH

Figure 4

(A)

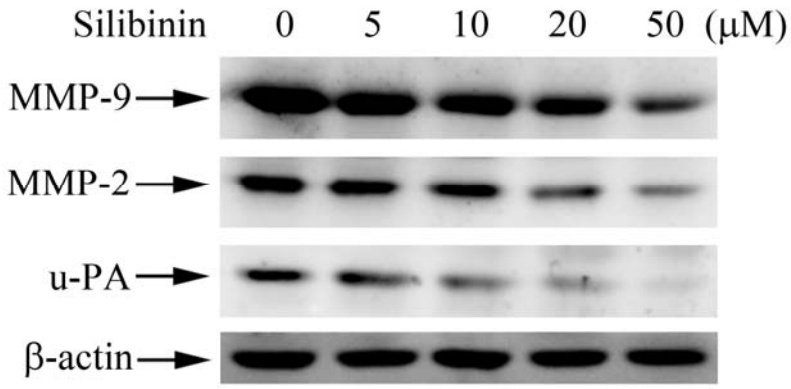
Silibinin 0 5 10 20 50 (μM)
MMP-9
MMP-2
u-PA
β-actin

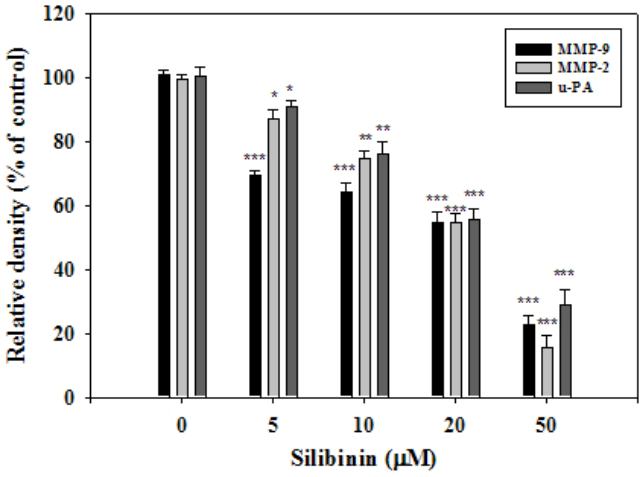
MMP-9
MMP-2
u-PA
Relative density (% of control)
Silibinin (μM)

(B)

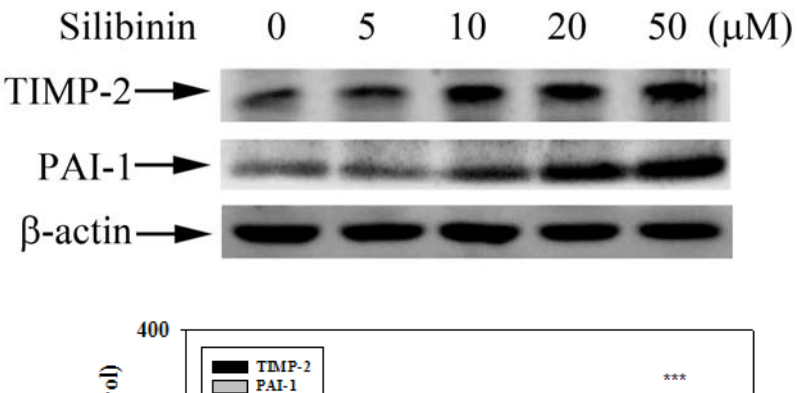
Silibinin 0 5 10 20 50 (μM)
TIMP-2
PAI-1
β-actin

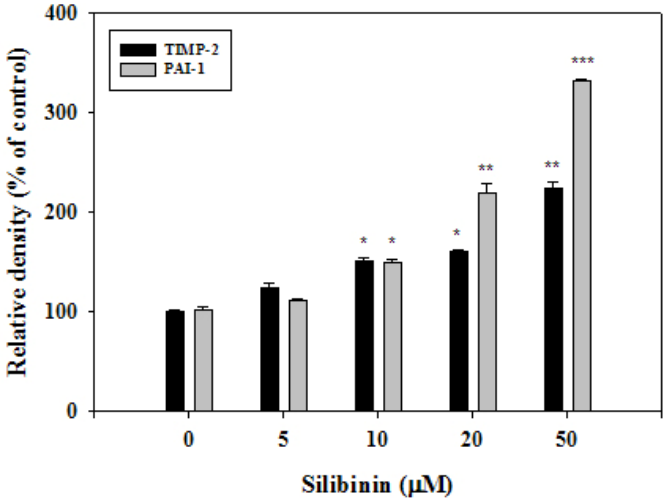
TIMP-2
PAI-1
Relative density (% of control)
Silibinin (μM)

Figure 5

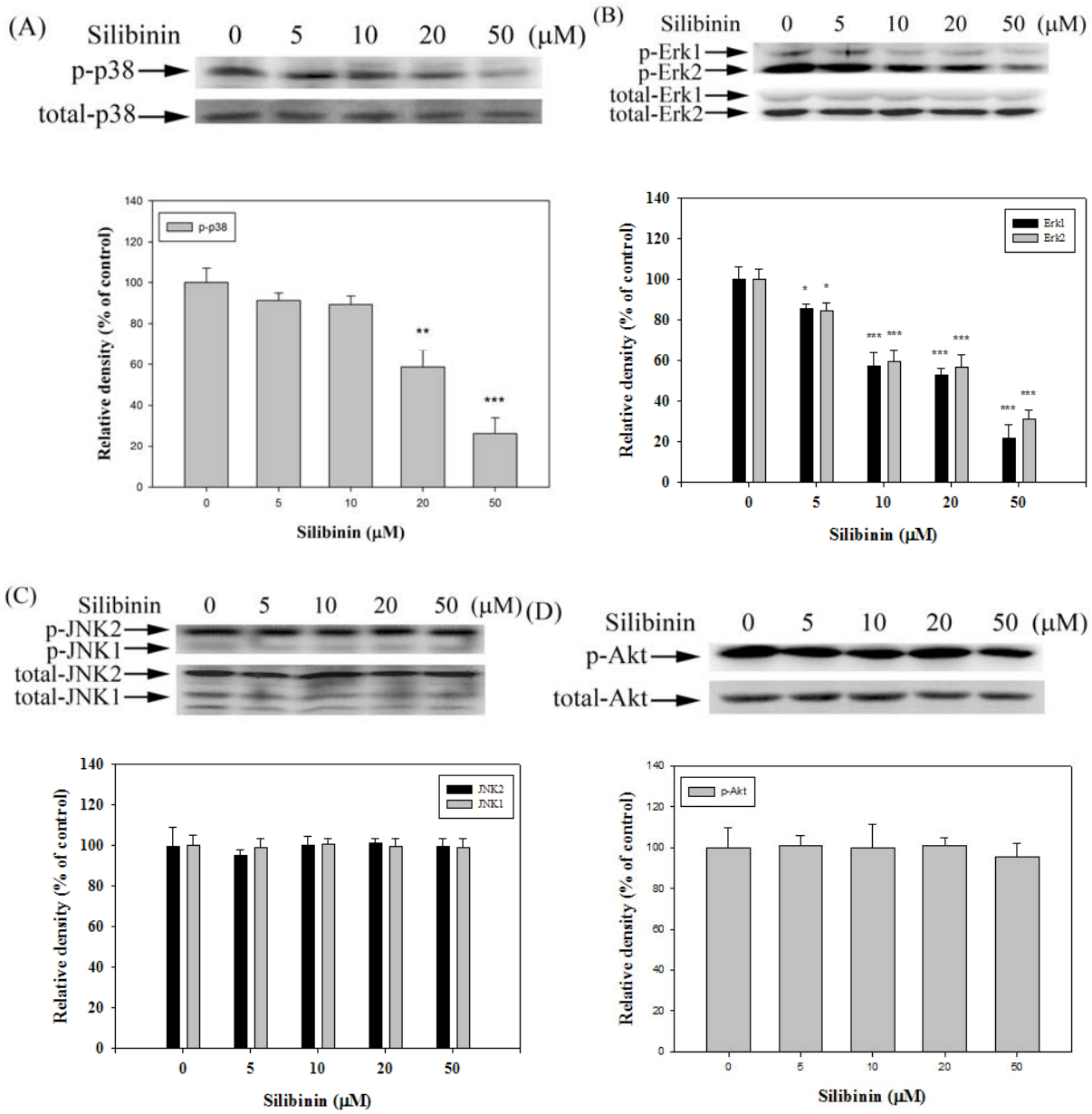
(A)
Silibinin 0 5 10 20 50 (μM)
p-p38
total-p38
(B)
Silibinin 0 5 10 20 50 (μM)
p-Erk1
p-Erk2
total-Erk1
total-Erk2
Relative density (% of control)
p-p38
Silibinin (μM)
Erk1
Erk2
(C)
Silibinin 0 5 10 20 50 (μM)
p-JNK2
p-JNK1
total-JNK2
total-JNK1
JNK2
JNK1
(D)
Silibinin 0 5 10 20 50 (μM)
p-Akt
total-Akt
p-Akt

Figure 6

(A)

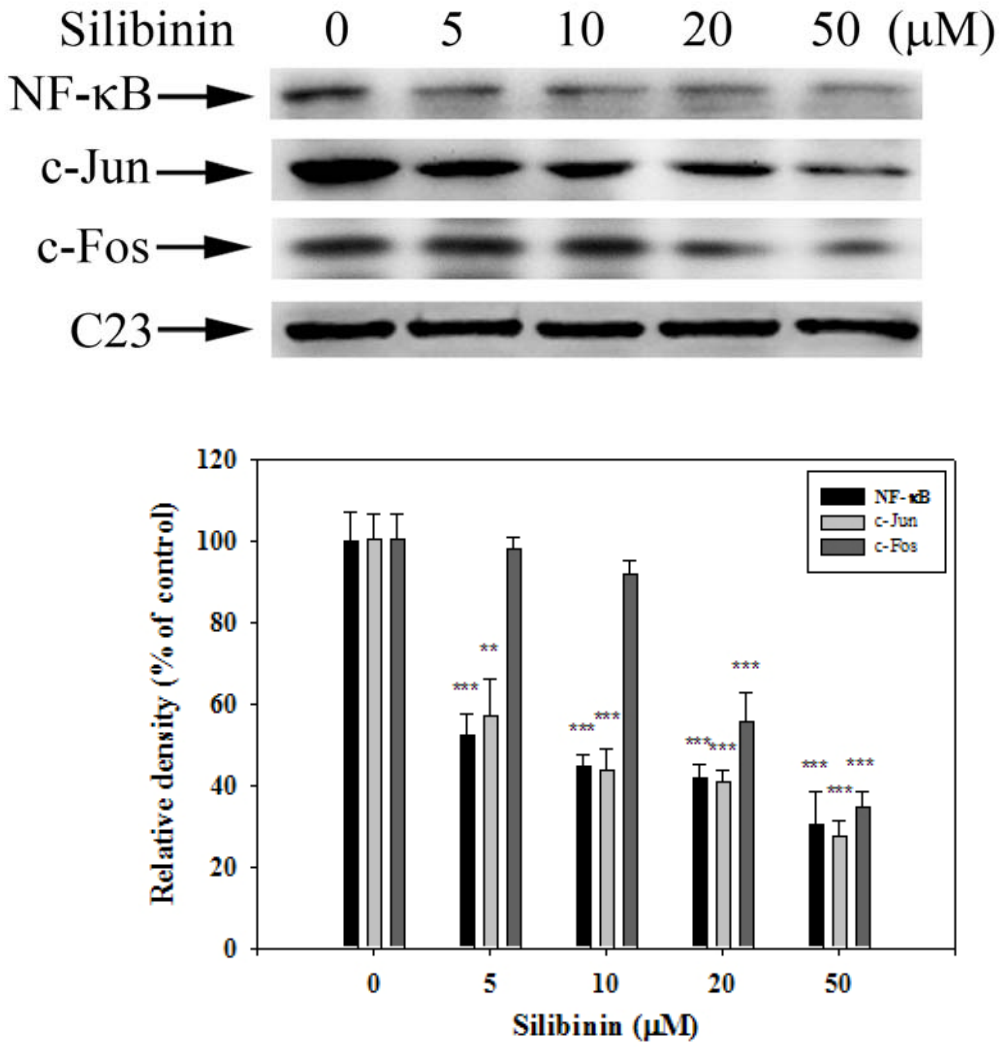
Silibinin 0 5 10 20 50 (μM)
NF-κB
c-Jun
c-Fos
C23
Relative density (% of control)
120
100
80
60
40
20
0
NF-κB
c-Jun
c-Fos
0
5
10
20
50
Silibinin (μM)

(B)

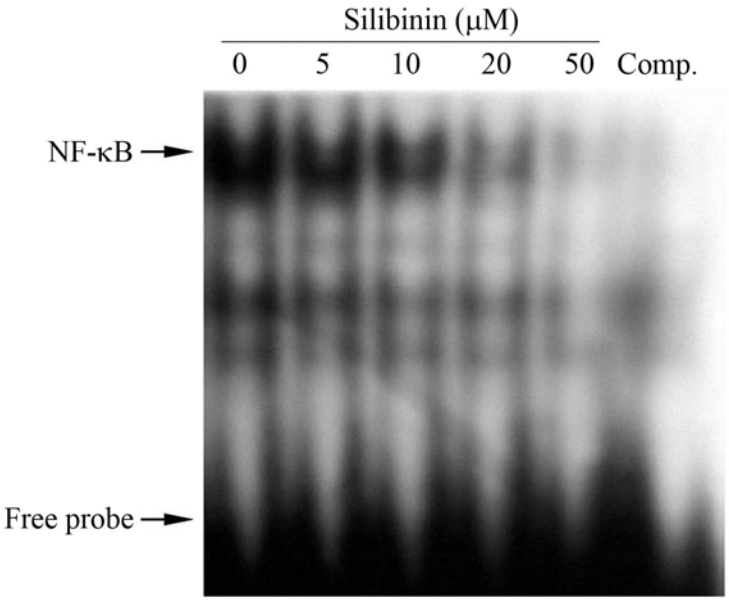
Silibinin (μM)
0
5
10
20
50
Comp.
NF-κB
Free probe

(C)

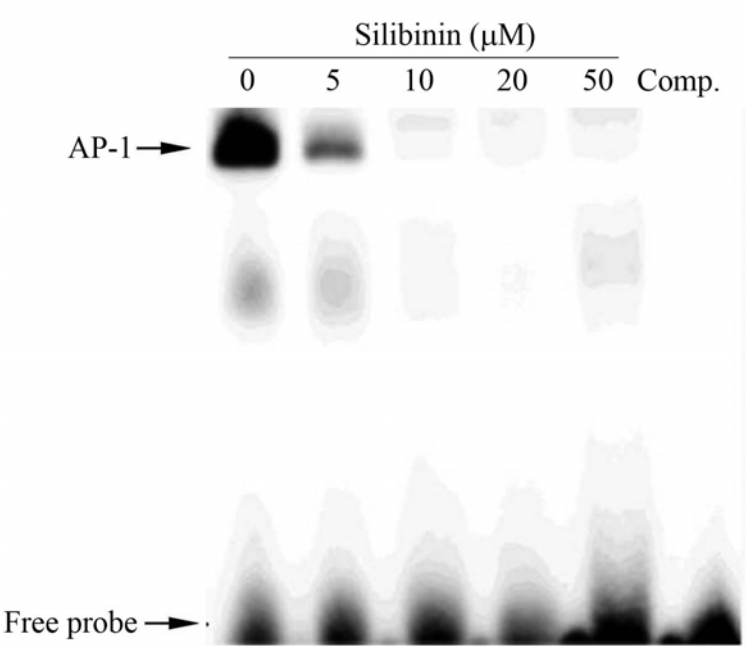
Silibinin (μM)
0
5
10
20
50
Comp.
AP-1
Free probe

Figure 7

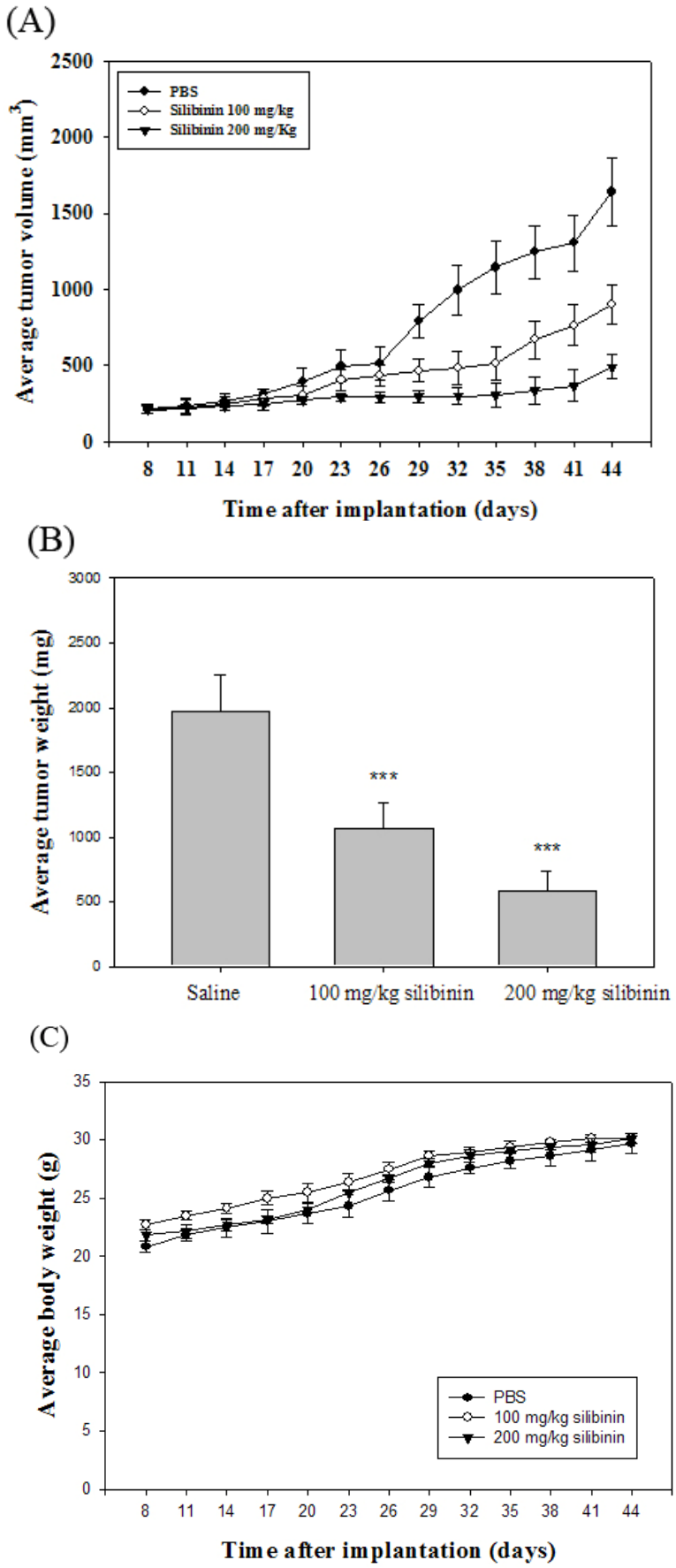
(A)
Average tumor volume (mm3)
PBS
Silibinin 100 mg/kg
Silibinin 200 mg/Kg
Time after implantation (days)
(B)
Average tumor weight (mg)
***
***
Saline
100 mg/kg silibinin
200 mg/kg silibinin
(C)
Average body weight (g)
PBS
100 mg/kg silibinin
200 mg/kg silibinin
Time after implantation (days)